

Aggregation of Expanded Polyglutamine Domain in Yeast Leads to Defects in Endocytosis

Anatoli B. Meriin,¹ Xiaoqian Zhang,¹ Nicholas B. Miliaras,² Alex Kazantsev,³
Yury O. Chernoff,⁴ J. Michael McCaffery,^{2,5} Beverly Wendland,²
and Michael Y. Sherman^{1*}

Department of Biochemistry, Boston University School of Medicine,¹ and Department of Neurology, Massachusetts General Hospital,³ Boston, Massachusetts; Department of Biology² and The Integrated Imaging Center,⁵ The Johns Hopkins University, Baltimore, Maryland; and School of Biology and Institute for Bioengineering and Bioscience, Georgia Institute of Technology, Atlanta, Georgia⁴

Received 4 June 2003/Returned for modification 15 July 2003/Accepted 25 July 2003

The role of aggregation of abnormal proteins in cellular toxicity is of general importance for understanding many neurological disorders. Here, using a yeast model, we demonstrate that mutations in many proteins involved in endocytosis and actin function dramatically enhance the toxic effect of polypeptides with an expanded polyglutamine (polyQ) domain. This enhanced cytotoxicity required polyQ aggregation and was dependent on the yeast protein Rnq1 in its prion form. In wild-type cells, expression of expanded polyQ followed by its aggregation led to specific and acute inhibition of endocytosis, which preceded growth inhibition. Some components of the endocytic machinery were efficiently recruited into the polyQ aggregates. Furthermore, in cells with polyQ aggregates, cortical actin patches were delocalized and actin was recruited into the polyQ aggregates. Aggregation of polyQ in mammalian HEK293 cells also led to defects in endocytosis. Therefore, it appears that inhibition of endocytosis is a direct consequence of polyQ aggregation and could significantly contribute to cytotoxicity.

Special mechanisms of refolding and selective degradation have evolved to protect cells from accumulation of mutant and damaged polypeptides. If these cellular mechanisms fail, the abnormal proteins aggregate, often forming large inclusion bodies (IBs) (for a review, see reference 41). It was initially assumed that protein aggregation is a spontaneous process, resulting from a natural tendency of unfolded polypeptides to associate with each other. However, recently it became clear that intracellular protein aggregation is a complex process which involves a number of cellular elements. In the cytoplasm of mammalian cells, small aggregates often converge via microtubule-based transport to the centrosome and recruit heat shock proteins and components of the ubiquitin-proteasome degradation pathway to form the so-called aggresome (1, 13, 14, 19, 53, 58, 60). Furthermore, formation of IBs is regulated by cellular signaling proteins, including the stress-activated kinase MEKK1 (24), the GTP-binding protein regulator arfap-2 (34), steroid hormones (11), and the Akt kinase pathway (18, 29).

The mechanism of intracellular protein aggregation attracts much attention because of its relevance to a number of known pathological conditions. In many major neurodegenerative diseases, such as amyotrophic lateral sclerosis, Alzheimer's disease, Parkinson's disease, and Huntington's disease, the pathology and the eventual death of specific neuronal populations occur as a result of accumulation of specific abnormal polypeptides. These polypeptides can aggregate and form in-

soluble intracellular inclusions (41). The formation of the IBs generally precedes neurodegeneration and cell death (62). Such observations initially led to the widely held assumption that aggregate formation is the critical event triggering neuropathology at least in some of these diseases (see below). Although the role of intracellular aggregates of abnormal proteins in neurodegeneration has not been clarified yet, there have been a number of hypotheses about potential mechanisms of cell toxicity mediated by IBs. For example, it was shown that the appearance of protein aggregates in cytosol correlates with a general cessation of the ubiquitin-proteasome pathway of protein degradation (5, 16). It was suggested that this cessation is due to entrapment of proteasomes and other components of the pathway within the IBs (5). It was also found that formation of IBs often correlates with inhibition of several transcription programs, probably due to abnormal association of certain transcription factors with IBs (32, 45, 46). In all of these models, however, there was no clear connection between formation of IBs and cell toxicity. Here, we address the deleterious effects of protein aggregation by using a recently developed yeast model of polyglutamine (polyQ) expansion disorders (25).

A group of neurodegenerative disorders, including Huntington's disease, are associated with genetic expansion of polyQ domains in certain proteins. polyQ expansion causes mutant polypeptides (e.g., huntingtin) to acquire an unusual conformation, which facilitates their aggregation into intracellular IBs and causes cell toxicity (4, 12, 39). The question of whether toxicity and neurodegeneration are caused by soluble polyQ-containing proteins or by IBs has been the focus of debate in the field for a number of years, since available data with cellular and animal models are indirect and often controversial

* Corresponding author. Mailing address: Boston University School of Medicine, Department of Biochemistry, K323, 715 Albany St., Boston, MA 02118. Phone: (617) 638-5971. Fax: (617) 638-5339. E-mail: sherman@biochem.bumc.bu.edu.

TABLE 1. Strains

Strain	Genotype	Source
W303	<i>MATa ade2-1 trp1-1 leu2-3,112 his3-11,15 ura3-52 can1-100 ssd1-d</i>	S. Lindquist
<i>hsp104Δ</i> mutant (YS483)	<i>hsp104::LEU2</i> ; isogenic with W303	S. Lindquist
NMY75	<i>MATα ADE2</i> ; isogenic with W303	B. Wendland
SEY6210	<i>MATα his3 trp1 leu3 ura3 lys2</i>	S. Emr
SEY6210a	<i>MATa leu2 ura3 trp1 his3 lys2</i>	S. Emr
BWY1348	<i>end3-1</i> ; result of three consecutive crosses of <i>end3-1</i> mutant with SEY6210	B. Wendland
BWY1237	Isogenic with SEY6210; <i>pan1-20</i>	B. Wendland
DDY0131	<i>ade2 his3Δ200 leu2-3,112 lys2-801 ura3-52</i>	D. Drubin
DDY1166	<i>sla2::HIS3</i> ; isogenic with DDY0131	D. Drubin
GW047	<i>MATa rsp5::LEU ade2 ura3 his3</i> [pRS414-RSP5-HA]	J. Huibregtse
JCY459	<i>MATa leu2 his4 ura3 bar1</i>	H. Riezman
RH2607	<i>end8-1</i> ; isogenic with JCY459	H. Riezman
RH2615	<i>end9-1</i> ; isogenic with JCY459	H. Riezman
RH2618	<i>end10-1</i> ; isogenic with JCY459	H. Riezman

(for a review, see reference 41). On the other hand, our yeast model, which reproduces both polyQ length-dependent aggregation and toxicity, demonstrates a clear connection between the two processes. Furthermore, it allows genetic investigation of which cellular components are involved in protein aggregation and what effects IBs have on cellular metabolism. When expressed under control of the *GAL1* promoter, a fragment of huntingtin carrying the N-terminal 17-amino-acid stretch followed by a normal polyQ domain (25Q) did not form IBs in yeast cells, while a fragment containing expanded polyQ (103Q) aggregated in every cell (25). In contrast to the case for 25Q, accumulation of 103Q in yeast cells was toxic, so 103Q-expressing cells plated on selective galactose media formed only small colonies.

Aggregation of polyQ-containing polypeptides in yeast depends on the prion conformation of yeast prion-like proteins (25, 33). The prion form of Rnq1 protein ([RNQ⁺]), which was shown recently to be essential for switching to the prion form of other yeast prion-like proteins (10, 33), plays a critical role in the initial steps in aggregation of polyQ. In fact, either deleting *RNQ1* or changing the conformation of this protein into a nonprion form led to suppression of aggregation of 103Q (25) or another polyQ-containing protein, MJD (33). Suppression of aggregation by *mq1Δ* and a number of other mutations or by curing of [RNQ⁺] inhibited the toxicity of expanded polyQ in this model (25), indicating that the toxicity is intimately associated with the 103Q aggregation.

Here we extended our search for cellular factors involved in development of toxicity of polypeptides with expanded polyQ. We found that several genes required for early endocytic events and organization of cortical actin patches also enhanced 103Q toxicity when deleted or mutated, allowing us to establish a connection between the polyQ-mediated toxicity and inhibition of early steps of endocytosis.

MATERIALS AND METHODS

Strains and plasmids. Deletion mutants of the wild-type strains BY4739 (*MATα leu2Δ lys2Δ ura3Δ*), BY4742 (*MATα his3Δ leu2Δ lys2Δ ura3Δ*), and BY4741 (*MATa his3Δ leu2Δ met15Δ ura3Δ*) (used only with *mq1Δ* and *vps34Δ*) were obtained from the deletion library (ResGen; Invitrogen) of yeast nonessential genes (59). All other strains used in this work are listed in Table 1.

HEK293 (human embryonic kidney) cells were grown in Dulbecco's modified Eagle medium supplemented with 10% fetal bovine serum at 37°C in an atmosphere of 5% CO₂. For transfection, HEK293 cells were grown in 35-mm-

diameter dishes to 25 to 50% confluence and then were transfected for 1.5 h with GenePORTER reagent (Gene Therapy Systems, San Diego, Calif.) in accordance with the manufacturer's protocol, using 18 μl of the reagent and 3 μg of vector per dish.

The pYES2-based vector for expression of green fluorescent protein (GFP)-tagged polyQ constructs under control of the *Gall* promoter was described previously (25). To tag the constructs with cyan fluorescent protein (CFP) instead of GFP, the *BamHI-XbaI* gene fragment of the construct was replaced with the analogous fragment of the CFP gene. For mammalian expression, the whole GFP-tagged polyQ constructs were inserted in plasmid pCDNA3.1(+) under control of the constitutive cytomegalovirus promoter. The vector for expression of glutathione *S*-transferase (GST) [pEG(KT)] was described before (28). The vector for expression of GFP-tagged Ste6 from its own promoter (pSM1181) was a gift of S. Michaelis (Johns Hopkins Medical School, Baltimore, Md.).

Observation of yeast growth and induction. Cells were routinely (unless indicated otherwise) grown at 30°C on selective minimal medium with glucose and then transferred into liquid or solid selective minimal medium with galactose for induction of 25Q or 103Q at the same temperature. To compare the timings of 103Q-dependent effects on endocytosis and on cell growth (see Fig. 2B), cell cultures were grown in selective liquid media with 2% raffinose and polyQ synthesis was induced by addition of 2% galactose (2% more of raffinose was added to noninduced control cells).

Transformed cells were routinely single-colony purified on selective plates with glycerol to select against petite mutants.

Curing of prions by guanidine chloride (GuHCl) treatment was described before (25).

Microscopy. Fluorescence microscopy was performed with an Axiovert 200 (Carl Zeiss) microscope with a 100× objective.

For staining with FM4-64 (Molecular Probes), mid-log-phase cells expressing polyQ were concentrated 10 times and incubated with 8 μM dye (5 mM FM4-64 in dimethyl sulfoxide was diluted with water to obtain a 400 μM stock solution) for 12 min in the selective medium with galactose. Cells were either immediately observed under a microscope or washed two times with the same medium and left in it for the indicated time periods. Fluorescence of GFP in nonfixed yeast cells (in sharp contrast with fixed cells) leaked into the red channel in a nonlaser fluorescence microscope (the red particles colocalized perfectly with 103Q aggregates and were seen in the absence of FM4-64 treatment [not shown]), overlapping with the signal of FM4-64. To avoid such an overlap in Fig. 2A, we replaced GFP in the 103Q and 25Q constructs with CFP, whose emission spectrum is more distant from that of FM4-64; the substitution did not impair 103Q toxicity (not shown).

For staining with Texas red-conjugated phalloidin (Molecular Probes), mid-log-phase cells expressing polyQ were fixed for 75 min with 4% formaldehyde in 100 mM potassium phosphate (pH 6.5), washed twice with phosphate-buffered saline (PBS) and permeabilized with 0.2% Triton X-100 for 15 min. The cells were washed twice again, labeled with the dye (20 U/ml in PBS) for 1 h, and, after four washes, observed under the microscope.

For immunostaining, cells expressing polyQ were fixed with 4% formaldehyde for 20 min in the medium and then for 50 min in 50 mM potassium phosphate (pH 6.5)–0.5 mM MgCl₂, washed twice, and incubated at 37°C for 50 min with 40 μg of Zymolyase per ml in the same buffer supplemented with 1.2 M sorbitol and 0.3% 2-mercaptoethanol. The cells were then washed twice, permeabilized with

0.2% Triton X-100 for 45 min in PBS with 3% bovine serum albumin, washed twice, and incubated with appropriate primary and secondary antibodies. Electron microscopy was done as described previously (38).

Ste3 degradation assay. NMY75 cells transformed with either the p(EG) KT, 103Q(GFP), or 25Q(GFP) plasmid were grown at 30°C to early log phase in selective media supplemented with 4% raffinose. Cells were induced for 6 h by addition of galactose to a 3% final concentration. Cycloheximide was then added to 5 μ g/ml, and samples were collected at the indicated time points and immediately supplemented with 10 mM NaN₃ and 10 mM NaF on ice. Collected cells were disrupted by 5 min of vortexing with 425- to 600- μ m-diameter acid-washed glass beads in lysis buffer containing 0.4% sodium dodecyl sulfate (SDS), 2.5% 2-mercaptoethanol, and 6 M urea. After 5 min of denaturation at 70°C, extracts were subjected to immunoblotting and the relative intensities of Ste3 bands were digitally quantified by using Alpha Innotech software.

API maturation assay. Cells were grown in minimal selective media supplemented with 4% raffinose and polyQ constructs were induced with 3% galactose or repressed with 3% dextrose for 6 h at 30°C, then 5 OD₆₀₀ units of each strain were incubated for 4 h at 30°C in the same media or in nitrogen-free media, supplemented, respectively, with either galactose or dextrose. The samples were precipitated with 10% TCA, washed with acetone and treated with glass beads and the lysis buffer as in the Ste3p assay and then subjected to immunoblotting with anti-aminopeptidase I (anti-API) antibody.

Transferrin receptor endocytosis assay. At 20 h after transfection, cells were incubated for 40 min in Dulbecco's modified Eagle medium without serum and then for 15 min in the same medium containing 100 μ g of Texas red-conjugated transferrin (Molecular Probes) per ml. The cells were placed on ice, washed three times with cold PBS, fixed with 4% formaldehyde, washed, and observed with an Axiovert 200 microscope with a 40 \times objective.

Analysis of protein solubility in cell lysates. Collected cells were disrupted by 10 min of vortexing with 425- to 600- μ m-diameter acid-washed glass beads in lysis buffer (40 mM HEPES [pH 7.5], 50 mM KCl, 1% Triton X-100, 1 mM Na₂VO₄, 50 mM β -glycerophosphate, 50 mM NaF, 5 mM EDTA, 5 mM EGTA, 1 mM phenylmethylsulfonyl fluoride, 1 mM benzamidine, and 5 μ g each of leupeptin, pepstatin A, and aprotinin per ml). Homogenates were cleared by 5 min of centrifugation at 500 \times g. Samples were normalized by the amount of total protein and subjected to centrifugation at 10,000 \times g for 10 min. The resulting supernatant was subjected to centrifugation at 200,000 \times g. The pellets were washed once with the lysis buffer and solubilized with loading SDS-polyacrylamide gel electrophoresis buffer containing 2% SDS. The differential centrifugation assay for prion status of Rnq1 was described before (25).

Antibodies. Anti-GFP antibody (polyclonal) was from Clontech, and antihemagglutinin (anti-HA) antibodies were from Santa Cruz and Babco. Anti-Rnq1 antibody was a gift of S. Lindquist (Whitehead Institute, Massachusetts Institute of Technology, Cambridge), anti-Pan1 antibody was a gift of A. Sachs (University of California, Berkeley), and anti-Ste3p antibody was a gift of G. Payne (University of California, Los Angeles). Anti-API antibody was a gift of D. Klionsky (University of Michigan, Ann Arbor). Anti-yAP180 and anti-Ent1 antibodies were prepared by B. Wendland.

RESULTS

Mutations in genes encoding endocytic proteins enhance polyQ toxicity. Previously, using the yeast model of polyQ cytotoxicity, we have found that mutations in certain host cell genes required for propagation of [RNQ⁺] suppress the aggregation and toxicity of expanded polyQ (25). We then analyzed whether other mutations known to affect yeast prions can also affect polyQ toxicity, and we noticed that the growth of *sla1* Δ cells expressing 103Q was impaired to a greater extent than that of wild-type cells (Fig. 1, top). Importantly, the mutant cells expressing 25Q grew normally (Fig. 1, top), indicating that the *sla1* mutation does not cause the growth defect on its own but rather enhances the polyQ-related toxicity. These data were particularly intriguing since the Sla1 protein was previously shown to interact with extended polyQ in a two-hybrid screen (3). Sla1 plays a critical role in formation of actin patches, and dynamically associates with various proteins involved in early events of endocytosis (i.e., Pan1, Sla2, and

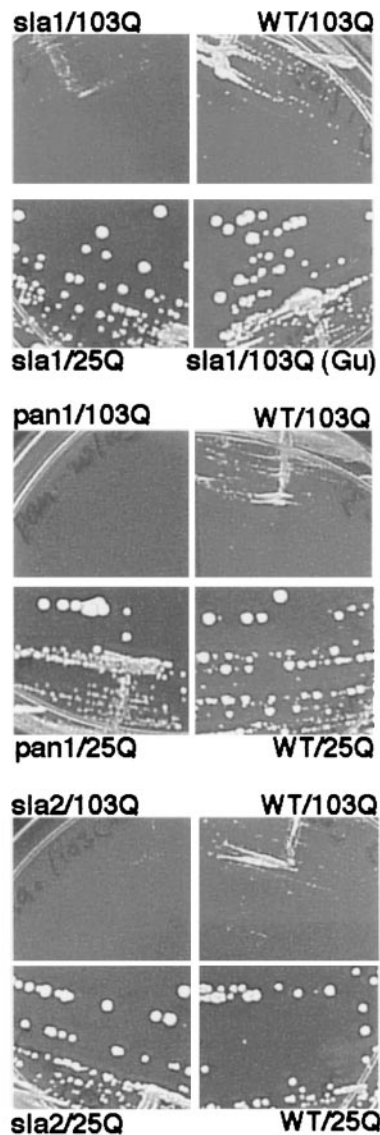


FIG. 1. The toxicity of expanded polyQ is enhanced by mutations affecting endocytosis. Mutant and respective wild-type (WT) strains transformed with either 25Q or 103Q constructs were plated on selective galactose media and grown for 4 days at 30°C (for the *sla1* mutant) or for 5 days at 25°C (for the *pan1* and *sla2* mutants). *sla1/103Q* (Gu), *sla1* mutant strain transformed with the 103Q construct and rescued from [RNQ⁺] prion by GuHCl treatment.

End3) (48, 55, 63). Therefore, we hypothesized that mutations in the genes encoding these proteins or other elements of the endocytic machinery may also have an effect on the polyQ toxicity. To test this hypothesis, we typically used deletion mutations in a number of genes involved in endocytosis. However, since *PAN1* is an essential gene, we utilized a *pan1*-ts mutant at the permissive temperature of 25°C. The mutant strains were transformed with plasmids encoding either 103Q or 25Q, controlled by a galactose-regulated promoter, and polyQ toxicity was tested by plating transformed cells on galactose selective media (Fig. 1 and Table 2).

As hypothesized, mutations in almost all of the tested genes,

TABLE 2. Effect of mutations associated with endocytosis on toxicity of 103Q

Gene ^a	Toxicity ^b
<i>abp1</i>	Same
<i>aip1</i>	-
<i>apm4</i>	Same
<i>ark1</i>	Same
<i>apl1</i>	-
<i>apl3</i>	Same
<i>bull1</i>	Same
<i>chc1</i>	--
<i>clc1</i>	--
<i>ede1</i>	-
<i>end3</i>	-
<u><i>end3-1</i></u>	-
<u><i>end8-1</i></u>	--
<u><i>end9-1</i></u>	--
<u><i>end10-1</i></u>	--
<i>end11</i>	--
<i>ent1</i>	Same
<i>ent2</i>	Same
<i>mkk2</i>	Same
<i>myo3</i>	Same
<i>pan1</i>	-
<i>pan2</i>	Same
<i>prk1</i>	Same
<i>rex3</i>	Same
<i>rvs161</i>	-
<i>rvs167</i>	-
<i>she4</i>	-
<i>sac6</i>	Same
<i>sjl1</i>	-
<i>sjl2</i>	Same
<i>sjl3</i>	Same
<i>sla1</i>	-
<i>sla2</i>	-
<i>srv2</i>	--
<i>vid31</i>	Same
<i>vma2</i>	Same
<i>vps11</i>	-
<i>vps13</i>	-
<i>vps15</i>	Same
<i>vps33</i>	Same
<i>vpr1</i>	-

^a Underlining indicates mutant genes; all others are deletions.

^b Same, toxic effect of 103Q expression is close to that seen with the wild type; -, mutant cells expressing 103Q form much smaller colonies than wild-type cells; --, almost no growth on selective galactose media.

with the exceptions of genes which are redundant in endocytosis (e.g., *ENT1* and *ENT2*), strongly enhanced the polyQ toxicity (Table 2). Some mutations that have not been reported to affect endocytosis but that are involved in organization of the actin cytoskeleton, such as *aip1*, also enhanced the toxicity. Remarkably, one of the mutations enhancing polyQ toxicity is in *SLA2* (Fig. 1 and Table 2), a yeast homolog of a mammalian gene encoding the huntingtin-binding protein Hip1 (20). This suggested that the interactions of polyQ-containing polypeptides with the endocytic machinery are conserved in evolution.

To investigate whether the enhanced polyQ toxicity in mutant cells is of the same nature as the toxicity in wild-type cells, we tested whether [RNQ⁺] was still required for the toxicity enhanced by either *sla1* or *end3* deletions. As described before (25, 33), loss of [RNQ⁺] after consecutive passages on plates with 5 mM GuHCl suppresses polyQ aggregation in wild-type cells. *sla1* and *end3* deletion mutants were cured of [RNQ⁺] by

this procedure, so that Rnq1 became soluble in these clones as judged by differential centrifugation (not shown), and then were tested for polyQ-induced toxicity. As with wild-type cells, switching Rnq1 to the nonprion state suppressed the polyQ toxicity, and accordingly, large colonies that were similar in size to the colonies formed by [rnq⁻] wild-type cells grew on a selective galactose plate (shown for *sla1* in Fig. 1, top; not shown for *end3*). These data indicate that, as for polyQ toxicity in wild-type cells, the enhanced polyQ toxicity in the mutants requires [RNQ⁺]-dependent aggregation of polyQ.

Expanded polyQ inhibits endocytosis. Genetic interaction between 103Q and various components of the endocytic machinery hinted that emergence of expanded polyQ in a cell may on its own affect endocytosis. To test this possibility, we monitored the effect of polyQ expression on endocytosis by using the lipophilic fluorescent dye FM4-64 (52). This dye binds to the cell membrane and is internalized through the endocytic pathway, allowing us to monitor endocytosis by microscopy. Cells expressing 25Q (here tagged with CFP) demonstrated an FM4-64 labeling pattern characteristic of normal endocytosis: red patched structures, representing labeled endosomes, were seen in the cytoplasm within the first 10 to 15 min after the dye was added (Fig. 2A, top panels). At later times (60 min), the distinct ring-shaped labeling of the vacuoles was seen, reflecting fusion of the endosomes with vacuolar membrane. In striking contrast, almost none of 103Q-expressing cells contained either labeled endosomes or fluorescent rings surrounding vacuoles (Fig. 2A, bottom panels), indicating that accumulation of 103Q dramatically reduces the endocytosis of lipids in yeast cells. It is noteworthy that in 103Q-expressing cells, FM4-64 accumulated at the plasma membrane and was seen as rings surrounding cells (12 min) before being washed away. These data suggest that an early internalization step of endocytosis was affected.

Could the observed suppression of endocytosis represent a general slowdown of cellular metabolism due to 103Q accumulation? To address this question, we compared the time courses of 103Q effects on both endocytosis and cell growth. Cells were grown in raffinose-containing medium until mid-log phase, and 103Q synthesis was initiated immediately by addition of galactose to the growing cells. As seen in Fig. 2B, strong inhibition of FM4-64 internalization was seen in about 60% of cells after only 2 h of 103Q induction. In contrast, cell growth reduction could be detected more than 4 h after induction of 103Q. Later, during the course of 103Q synthesis, the growth rate continued to become lower, and after 24 h the induced culture with 103Q, while continuing to grow slowly, reached only 1/10 of the density of the noninduced culture (not shown). Therefore, inhibition of endocytosis by 103Q precedes general cessation of growth, and thus the endocytosis defect cannot be an indirect consequence of cell death.

To further investigate how specific are the effects of expanded polyQ on endocytosis, we performed electron microscopy of cells expressing polyQ constructs for 6 h. As seen in Fig. 2D, both in cells with 25Q and in cells with 103Q, cellular structures, including endoplasmic reticulum, mitochondria, and nuclei, looked normal. Remarkably, strong abnormalities seen in cells expressing 103Q, but not 25Q (Fig. 2D, panels Db to De), were associated with alterations of the vesicular transport pathway. We observed atypical tubular invaginations of

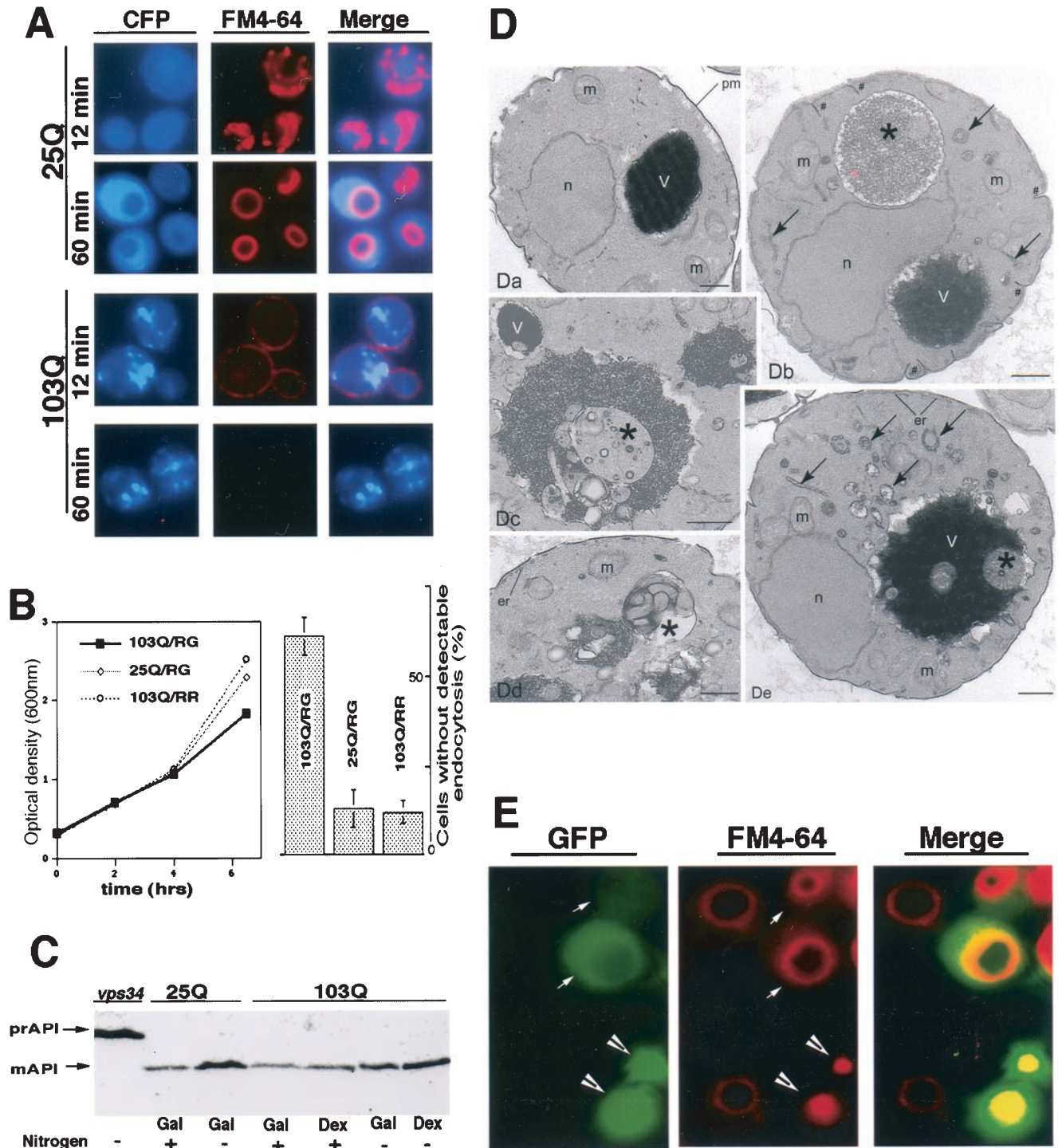


FIG. 2. Expression of expanded polyQ in yeast cells promptly suppresses lipid endocytosis. (A) Transformed W303 wild-type cells expressing CFP-tagged 25Q or 103Q (DAPI [4',6'-diamidino-2-phenylindole] channel) were stained with FM4-64 (Texas red channel) for 12 or 60 min (see Materials and Methods). In this experiment, for the clarity of images obtained with the wild-type cells we employed 103Q and 25Q constructs with GFP replaced by CFP (see Materials and Methods). (B) Endocytosis suppression precedes 103Q-dependent growth inhibition. In this experiment, to avoid a lag time due to a switch from dextrose, cells were grown in raffinose and induced by addition of galactose (see Materials and Methods). 103Q/RG and 25Q/RG, cells induced to synthesize 103Q and 25Q, respectively; 103Q/RR, noninduced cells in raffinose. Left panel, growth curves for the indicated cell cultures; right panel, more than 200 cells from each culture were assayed for lipid endocytosis 2 h after the induction. Error bars indicate standard deviations. (C) 103Q expression does not affect autophagy measured by a vacuolar cleavage of API precursor (prAPI). Galactose-induced (Gal) and noninduced (Dex) cells were incubated with (+) or without (-) a nitrogen source, extracted, and immunoblotted with anti-API antibody. Sample of cells with the *vps34* mutation, which disrupts autophagy, were used as a negative control to mark the position of prAPI in respect to processed (mAPI) protein. (D) Electron microscopy of cells expressing 25Q and 103Q. Panel Da, conventional electron microscopy of 25Q cells shows essentially normal morphology. Panels Db to De, conventional electron microscopy of 103Q cells shows unaffected

the plasma membrane, suggestive of internalization defects (Fig. 2D, panel Db). Also, aberrant cytoplasmic accumulations of vesicular structures representing putative endocytic intermediates (Fig. 2D, panels Db and De) were clearly seen. These structures are similar to endocytic intermediates that accumulate in *pan1* mutants (57) and probably result from a backup of the entire vesicular transport pathway due to the endocytosis defects (57). The abnormal vacuolar morphology, including the appearance of electron-translucent vacuolar and juxtavacuolar inclusions (Fig. 2D, panels Db to De), may indicate malfunction of later endocytic events.

Interestingly, autophagy, another cellular process that converges on the vacuole (for a review, see reference 31), remained unaffected in yeast cells experiencing 103Q-related toxicity. Indeed, as seen in Fig. 2C, proteolytic cleavage of the API precursor was not affected by 103Q expression. API, the yeast vacuolar enzyme, is synthesized in the cytoplasm as a precursor which is processed upon delivery to the vacuole either by autophagy (in nitrogen-starved cells) or by a parallel cytoplasm-to-vacuole targeting pathway (in nonstarved cells) (2). Thus, the fact that the processing of the API precursor remained unaffected demonstrates that transport of vesicles from the cytoplasm to the vacuole was not hindered by toxic 103Q and also suggests that the inhibition of endocytosis is not a result of indiscriminate metabolic slowdown in cells with polyQ aggregates.

To investigate whether aggregation of polyQ was critical for the inhibition of endocytosis, we analyzed this process in *hsp104* Δ cells expressing 103Q. As reported previously, while 103Q does not aggregate and thus is not toxic in the majority of *hsp104* Δ cells, in 10 to 40% of the mutant cells one or few large compact aggregates do form, which causes cytotoxicity (25). We took advantage of this feature of *hsp104* Δ cells and investigated whether the endocytosis of FM4-64 is specifically affected only in aggregate-containing cells. For this experiment, we used the GFP-tagged 103Q. In contrast to the case for the CFP-tagged polypeptide, 103Q-GFP fluorescence in nonfixed yeast cells leaks to the red channel, so that the 103Q-containing aggregates were also seen as bright particles in this channel. This allowed juxtaposition of cells with aggregates and cells with suppressed internalization of red FM4-64 in the same field. As seen in Fig. 2E, after 60 min of FM4-64 labeling and chase nearly all cells without 103Q aggregates exhibited the red ring-like vacuolar pattern characteristic of normal endocytosis. By contrast, almost no internalization of FM4-64 could be detected in the cells with aggregates. Therefore, inhibition of lipid endocytosis is associated with aggregation of polyQ.

To investigate the effect of polyQ aggregation on the endocytosis of a specific membrane receptor, we studied degradation of Ste3, the receptor for α -factor mating pheromone. Nor-

mally Ste3 is internalized and degraded in vacuoles, and thus the half-life of Ste3 reflects the efficiency of endocytosis and transport to vacuoles (9). Accordingly, we inhibited protein synthesis in cells with cycloheximide and followed the kinetics of Ste3 degradation (Fig. 3A). The half-life of Ste3 in 25Q-expressing cells was about 20 min, which was similar to that in control cells expressing GST. In contrast, expression of 103Q strongly reduced the rate of Ste3 degradation, so that a 50% decrease in the Ste3 level was observed only after a 90-min chase, suggesting that 103Q expression inhibited endocytosis of the receptor (Fig. 3A). Importantly, an extended Ste3 half-life could already be detected after 3 h of 103Q expression (data not shown).

We also assayed the effect of polyQ expression on the internalization of another membrane protein, Ste6, the α -factor transporter (6). Ste6 tagged with GFP was coexpressed with 103Q-CFP, and its distribution in individual cells was observed. In wild-type cells, Ste6 is found primarily in intracellular compartments and the vacuole lumen, whereas in endocytosis mutants with defects in internalization, Ste6 accumulates at the plasma membrane. To juxtapose the signal from Ste6-GFP in the green channel and the signal from bright 103Q-CFP aggregates, which is also seen in this channel, we used *mq1* Δ cells, which, like *hsp104* Δ cells, rarely form a single compact 103Q aggregate (25). This allowed observation of Ste6-GFP distribution in the cell area not occupied by the aggregate. In 75% of 103Q-expressing *mq1* Δ cells without aggregates, Ste6-GFP localized mainly either to vacuoles or to cytosolic vesicular structures, which reflect various stages of Ste6 transport through the secretory and endocytic pathways (Fig. 3B). In sharp contrast, in about 75% of aggregate-containing cells with Ste6 expression, Ste6 was mostly retained at the plasma membrane, where it has a peripheral punctate distribution (Fig. 3B). Only 3% of the cells without aggregates displayed this feature (data not shown). Together, these data indicate that early steps of endocytosis are inhibited upon formation of 103Q aggregates.

Association of components of the endocytic machinery with polyQ aggregates. Since formation of polyQ aggregates led to inhibition of endocytosis, we hypothesized that some components of the endocytic machinery could be recruited into the polyQ aggregates. Initially, we assessed this recruitment by using the easily identifiable single large aggregates in *hsp104* Δ cells. We fixed 103Q-expressing *hsp104* Δ mutant cells and stained them with an antibody to Pan1, a scaffolding protein which associates with many endocytic proteins, e.g., Sla1, End3, yAP180A/B, and others (47, 56). In the absence of aggregates, Pan1 was distributed in cortical patches (47, 56), while in about 65% of cells with a single large polyQ aggregate, Pan1 associated with the aggregates (Fig. 4). Pan1 also colocalized with the smaller 103Q aggregates that form in wild-type

mitochondria (m), nuclei (n), and endoplasmic reticulum (er) but reveals aberrant cytoplasmic accumulation of putative endocytic intermediates (panels Db and De, arrows), atypical tubular invaginations of plasma membrane (pm) (panel Db, # [tubulations]), and abnormal vacuolar (V) morphology including electron-translucent vacuolar and juxtavacuolar inclusions (panels Db to De, * [vacuolar and juxtavacuolar inclusions]). Bars, 0.5 μ m. (E) *hsp104* Δ mutant cells expressing GFP-tagged 103Q (fluorescein isothiocyanate channel) assayed as described for Fig. 2A. Arrowheads point to cells with 103Q which formed an aggregate (seen also in the red channel as a particle); no rings characteristic of normal lipid endocytosis are formed in these cells. Cells containing only soluble 103Q (arrows) and cells with no detectable accumulation of 103Q (two cells on the left) both display unimpaired endocytosis.

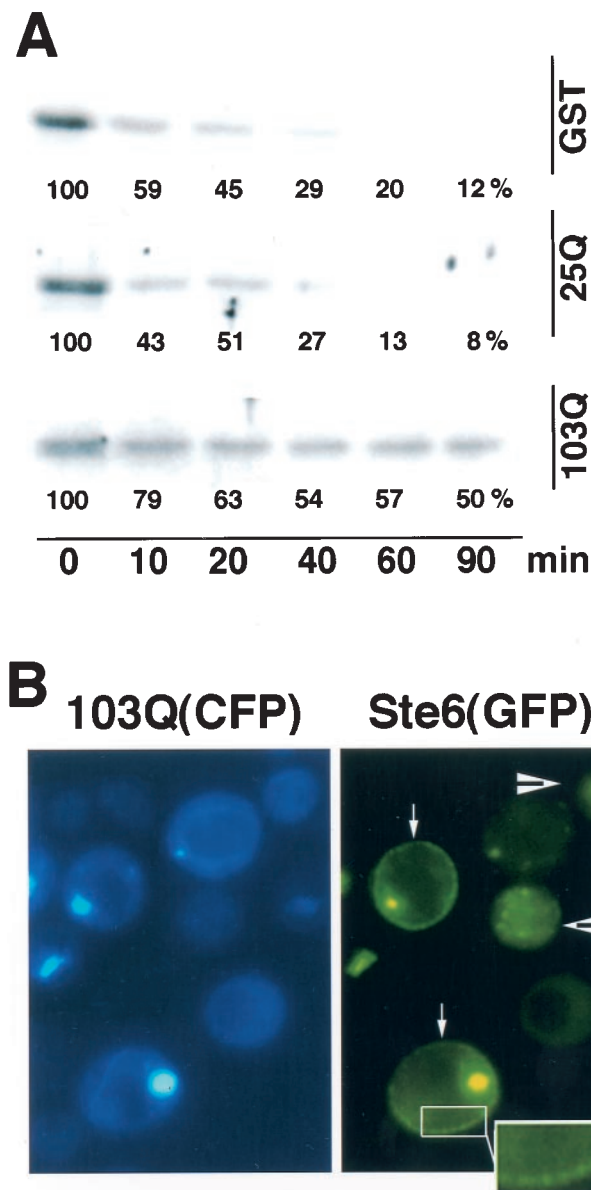


FIG. 3. Expression of expanded polyQ in yeast cells suppresses endocytosis of membrane receptors. (A) Suppression of Ste3 endocytosis. Cells expressing either GST, 25Q, or 103Q were induced for 6 h, after which total protein synthesis was blocked, and at the indicated time points samples were taken for immunoblotting with antibody against Ste3. The numbers under the bands represent their respective intensities. The experiment was independently reproduced three times. (B) Suppression of Ste6 endocytosis. *mq1Δ* (*MATa*) cells cotransformed with GFP-tagged Ste6 (constitutively expressed) and CFP-tagged 103Q were observed under a fluorescence microscope after 6 h of polyQ expression. Arrowheads point to cells with soluble 103Q, and arrows point to cells with an aggregate.

cells (data not shown). Since *PAN1* exhibits genetic interactions with *RSP5* (21), a gene encoding the E3 ubiquitin ligase involved in endocytosis of some membrane proteins (54), we also tested whether Rsp5 could be recruited into 103Q aggregates. For this experiment, we utilized a strain in which a plasmid encoding an HA-tagged Rsp5 complemented deletion

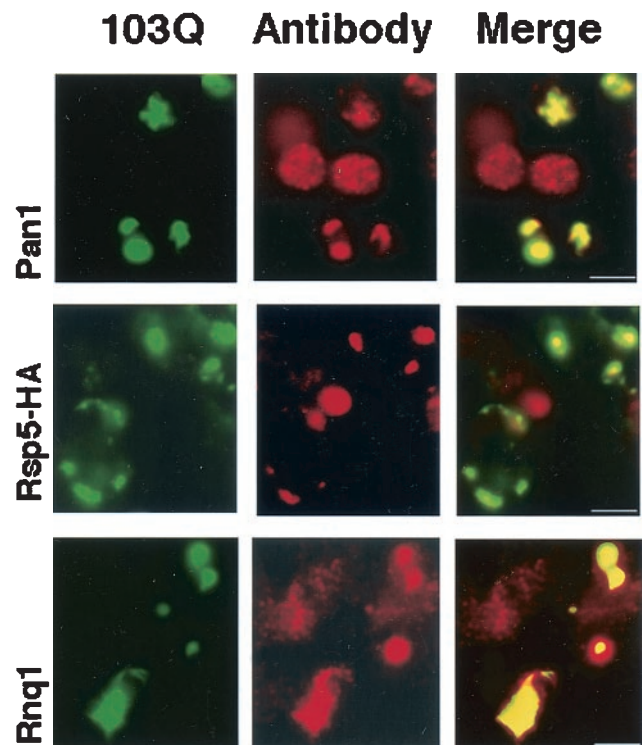


FIG. 4. Certain components of endocytosis machinery and Rnq1 associate with polyQ aggregates. Cells after overnight expression of 103Q (GFP tagged) were immunostained with an antibody (Texas red labeled) against the protein specified at the left of each row. In all images stained for Pan1 and Rsp5 *hsp104Δ* cells were used; Rsp5-HA was observed in strain GW047. Note that in contrast to the case for nonfixed yeast cells (Fig. 2), no GFP fluorescence is seen in the red channel after fixation. Bars, 4 μ m.

of endogenous *RSP5* (17). In these otherwise wild-type cells, 103Q expression caused Rsp5-HA to colocalize with the aggregates, as seen with anti-HA antibody staining (Fig. 4). The observed colocalization suggests formation of polyQ aggregates at the sites of endocytosis (thus physically perturbing this process) and/or recruitment of a critical component(s) of the endocytic machinery into 103Q aggregates.

The pattern of 103Q aggregates in wild-type cells is reminiscent of delocalized patches of cortical actin (61), suggesting a possible association of 103Q with these structures. This possibility is especially intriguing since some components of the endocytic machinery also function in organization of the actin cytoskeleton (for a review, see references 30 and 40). Furthermore, cortical actin patches (48, 55, 61, 63) have been suggested to be the sites of formation of endocytic vesicles (35). Normally the actin patches localize at the plasma membrane of the growing daughter cell (bud), but mutations in many endocytic proteins lead to delocalization of the patches (48, 61). Therefore, we studied whether polyQ aggregates colocalized with cortical actin patches by staining the latter with Texas red-conjugated phalloidin, a reagent specific for filamentous actin. For both wild-type and *hsp104Δ* mutant cells, in about 50% of aggregate-containing cells the phalloidin staining was seen mainly within 103Q aggregates (Fig. 5), suggesting a recruitment of actin into the aggregates. Colocalization of actin

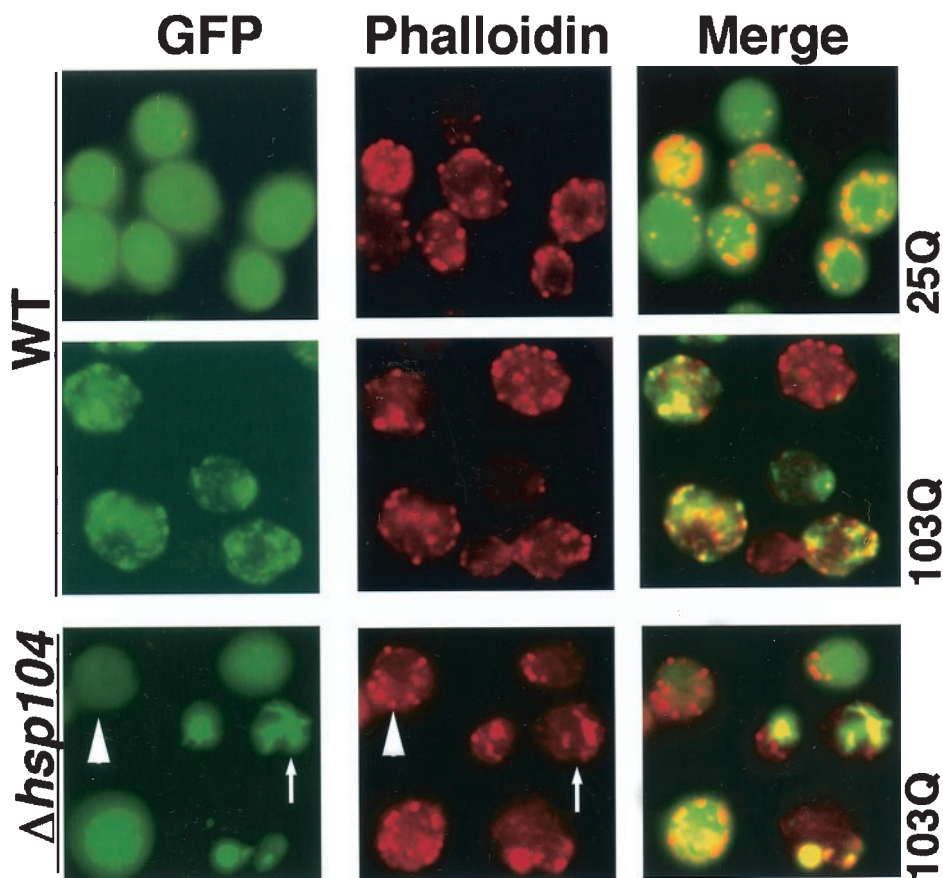


FIG. 5. Effects of polyQ aggregates on cortical actin. Fluorescence micrographs of wild-type (WT) or *hsp104* Δ cells fixed and stained with phalloidin (Texas red labeled) after 6 h of expression of either 25Q or 103Q are shown. The arrowhead points to a cell with soluble 103Q; the arrow points to a cell with an aggregate.

with polyQ-containing aggregates was also detected by immunogold labeling followed by electron microscopy (not shown). Furthermore, a large fraction of both wild-type cells and *hsp104* Δ cells with 103Q aggregates demonstrated either disappearance or delocalization of actin patches, consistent with a destabilized actin cytoskeleton.

Since high-throughput two-hybrid analysis demonstrated that Rnq1 can associate with some proteins of the endocytic pathway (see the database at <http://www.yeastgenome.org/>), and also due to the fact that the prion isoform of Rnq1 is essential for 103Q aggregation (25), we investigated whether this protein can itself associate with 103Q aggregates. Indeed, we found that Rnq1 clearly colocalized with 103Q aggregates not only in wild-type cells (not shown) but also in *hsp104* Δ cells (Fig. 4), suggesting that Rnq1 can directly interact with polyQ.

To assess quantitatively the effect of 103Q expression on the solubilities of Rnq1 and components of the endocytic machinery, we fractionated homogenates of yeast cells (prepared in the presence of 1% Triton X-100) by sequential differential centrifugations at $10,000 \times g$ (10 min) and $200,000 \times g$ (90 min). Pellets from each centrifugation (P10 and P200) were solubilized in SDS-containing buffer and analyzed along with the supernatant (S200) by immunoblotting with various antibodies. 103Q was found in both pellet fractions (Fig. 6A), while 25Q remained almost exclusively in a soluble fraction, as ex-

pected. In control cells, Pan1 was found mostly in the S200 fraction. Induction of 103Q expression caused redistribution of a significant fraction of Pan1 to the P10 fraction (Fig. 6B). This redistribution was accompanied by a partial depletion of Pan1 from the S200 fraction. Similarly, a fraction of yAP180A/B (not shown) and HA-tagged Rsp5 (Fig. 6B) were drawn into the P10 fraction upon expression of 103Q. By contrast, the Ent1/2 proteins were not redistributed to the P10 fraction upon expression of 103Q (Fig. 6B). These experiments indicated that certain components of the endocytic machinery are recruited into the polyQ aggregates and are partially depleted from the Triton X-100-soluble fraction. In fractions obtained from the control [RNQ⁺] cells, the vast majority of Rnq1 was in the P200 fraction (probably representing small Rnq1 aggregates), but upon expression of 103Q, a fraction of Rnq1 shifted to the heavier P10 fraction (Fig. 6C), likely through association with large polyQ aggregates. In *hsp104* Δ mutant cells, Rnq1 was present mostly in S200. However, upon expression of 103Q in *hsp104* Δ mutant cells, Rnq1 partially shifted to the P10 pellet (Fig. 6C), indicating that a significant fraction of Rnq1 is recruited into large aggregates in a subset of cells.

103Q-mediated inhibition of endocytosis in cultured mammalian cells. In order to investigate whether aggregation of polyQ can cause endocytosis defects in mammalian cells, we utilized HEK293 cells. Cells were transiently transfected with a

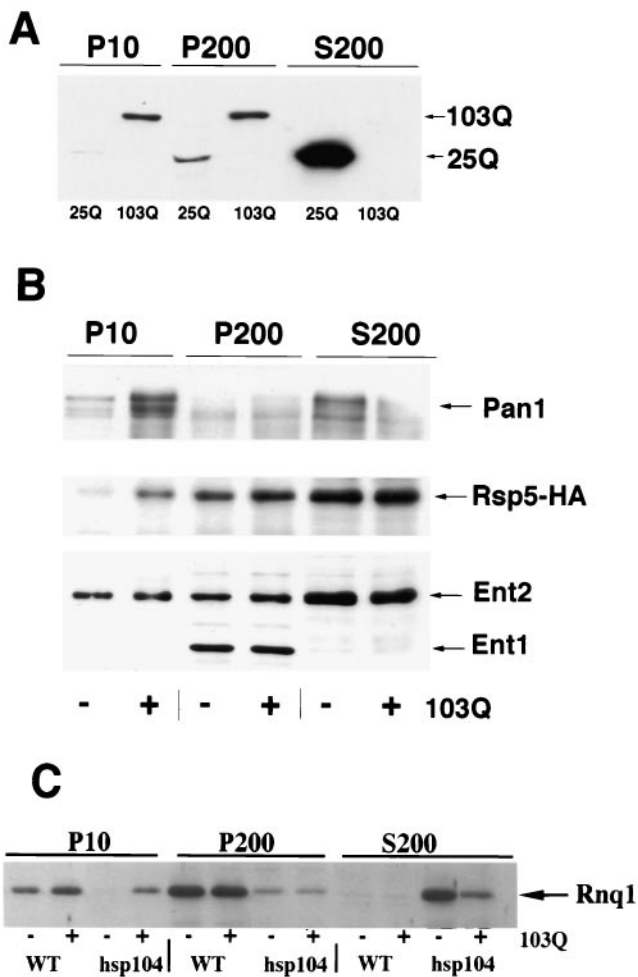


FIG. 6. Certain components of the endocytosis machinery and Rnq1 redistribute to a heavy particulate fraction in response to accumulation of expanded polyQ. Fractions resulting from consecutive centrifugations of precleared cellular homogenates were analyzed by immunoblotting with an antibody against GFP tag (A), against the protein specified for each blot (B), or against Rnq1 (C). P10, pellet after centrifugation at $10,000 \times g$ (10 min); P200 and S200, pellets and supernatants, respectively, after subsequent centrifugation at $200,000 \times g$ (90 min). Pellets were solubilized in half of the volumes of the respective supernatants in SDS-containing buffer. The immunoblots represent results from a typical experiment repeated three times. WT, wild type.

plasmid encoding 103Q-GFP. As described previously (24), at 20 h after transfection large polyQ aggregates were seen in 10 to 20% of the transfected cells, and the fraction of cells with aggregates continued to increase upon further incubation. At 20 h posttransfection, cells were incubated for 15 min with Texas red-tagged transferrin, which is internalized through receptor-mediated endocytosis (50) and is widely used as a standard marker for endosomal vesicles in cell cultures studies. Cells were washed, fixed, and observed by fluorescence microscopy. The internalized transferrin was seen as bright punctate structures in cytosol, corresponding to endosomes. Accordingly, the majority (about 75%) of cells without aggregates showed bright multiple transferrin-containing vesicles (Fig. 7). It is noteworthy that in transfected cells with only soluble

103Q, endocytosis remained unaffected in comparison with nontransfected cells (not shown). In contrast, in about 80% of cell with aggregates, both the number and brightness of such vesicles were strongly reduced, indicating suppressed endocytosis. These data show that aggregation of polyQ in mammalian cells can cause endocytosis defects, and therefore our findings with yeast could be relevant to human pathologies.

DISCUSSION

Aggregation of abnormal proteins, including polyQ-rich polypeptides, is often accompanied by entrapment of components of the ubiquitin-proteasome degradation pathway, chaperones, and certain transcription factors (5, 23, 32, 45, 46). This entrapment was suggested to suppress the respective metabolic processes. Here we present strong evidence that aggregation of polypeptides containing an expanded polyQ domain leads to defects in early steps of endocytosis, which clearly precedes the manifestation of polyQ-associated cell toxicity. Furthermore, the endocytosis appears to be affected rather specifically, since autophagy, another process involving vesicular transport to vacuoles, remained unobstructed and major cellular organelles observed by electron microscopy appeared unaffected. Moreover, the strong abnormalities seen on electron micrographs of cells with expanded polyQ (Fig. 2D) are closely reminiscent of ones associated with failed endocytosis (57). The suppression of endocytosis may be relevant to the toxicity, since in mutants with defects in the endocytic pathway, expression of polyQ was significantly more deleterious than in the wild-type cells, making some of the mutations synthetic lethal.

What are the connections between protein aggregation and endocytosis? The simplest hypothesis is that upon aggregation of polyQ, components of the endocytic machinery become trapped in IBs, thus depleting crucial elements. Additionally, polyQ might form small aggregates at sites of endocytosis and physically perturb the process. This mechanism is less likely, however, since in the *hsp104* Δ and *mq1* Δ mutants, endocytosis was specifically blocked in the cells with a single large polyQ aggregate. Considering that these aggregates form within minutes by trapping soluble 103Q molecules into a newly formed seed (25), it is difficult to imagine the direct physical interaction of such a seed with multiple preexisting endocytic complexes. Therefore, it is most likely that polyQ aggregation inhibits endocytosis by trapping limiting factors for endocytosis and disrupting cortical actin.

Interestingly, many proteins involved in endocytosis contain polyQ stretches, which may play an important role in interactions with 103Q. However, Sla1 and Sla2, which may also interact with polyQ, do not have polyQ stretches in their sequences. Sla2 does contain a small QN-rich region with similarities to those found in the yeast prion proteins, such as Rnq1 and Sup35 (27), and it is possible that such a QN stretch is sufficient for interaction with polyQ. On the other hand, surprisingly, Ent1 was not found in a complex with polyQ aggregates, although it associates with Pan1 and contains a polyQ sequence. This indicates that there are other sequence elements or proteins, in addition to the polyQ stretch, that regulate the specificity of interactions between polyQ and other proteins.

The majority of proteins involved in endocytosis are not

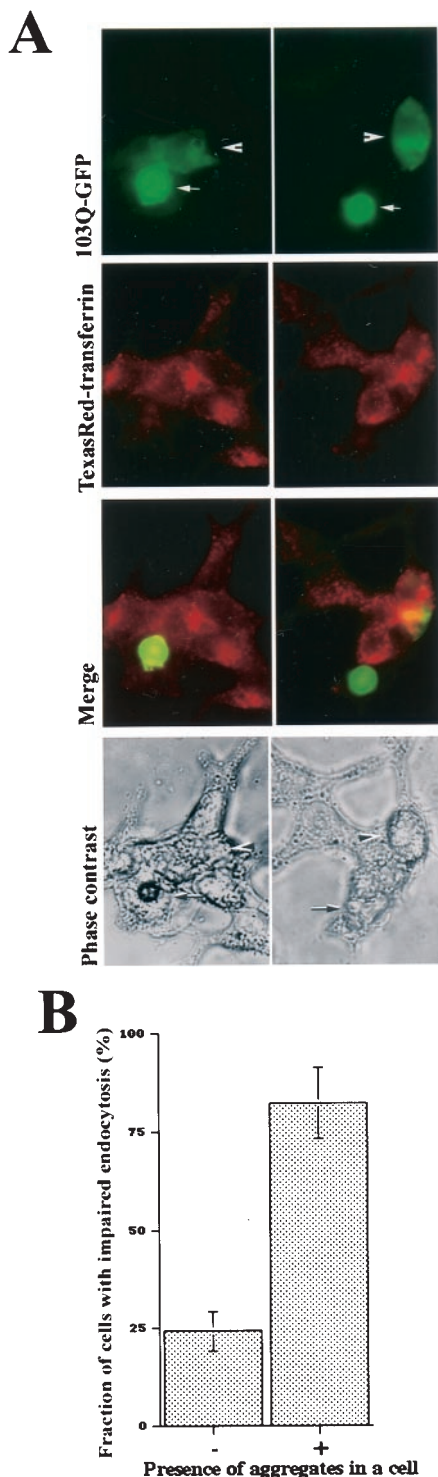


FIG. 7. polyQ aggregation in HEK293 cells suppresses endocytosis of transferrin receptor. (A) HEK293 cells transfected with 103Q after 15 min of incubation with Texas red-conjugated transferrin. Arrowheads mark transfected cells with soluble 103Q; arrows mark transfected cells with aggregated 103Q. (B) Assessment of endocytosis impairment in 335 randomly chosen cells as described for panel A. Error bars indicate standard deviations.

essential (e.g., End3, Sla2, and others). Therefore, either the depletion of an essential protein(s) (e.g., Pan1 or Rsp5) upon aggregation of polyQ is critical for the toxicity or partial depletion of multiple proteins results in a cumulative effect, inhibiting endocytosis and causing toxicity. We find the second possibility more likely because all of the proteins tested (i.e., Pan1, Rsp5, and yAP180A/B) were only partially depleted in the cells with aggregates. Importantly, two-hybrid analysis demonstrated that Rnq1 can interact with other components that exhibit genetic interactions with Pan1 (e.g., Rsp5 and Sjl2 [see the database at <http://www.yeastgenome.org/>]). Therefore, some components of the endocytosis machinery could be trapped in aggregates through direct interactions with polyQ, while others could be sequestered through interactions with Rnq1.

As reported previously, polyQ aggregation in yeast normally requires Rnq1 to be in the prion conformation (25, 33), although [PSI⁺] prion (G. Newnam and Y. Chernoff, unpublished observation) or [NU⁺] prion (33) could substitute for [Rnq⁺] in polyQ aggregation. It is conceivable that Rnq1 prion normally serves as a nucleation site for polyQ aggregation. However, if the prion conformation of Rnq1 is lost (in *hsp104Δ* cells), polyQ can still form a single large aggregate in a small fraction of cells. In these cells, Rnq1 nevertheless is recruited into polyQ aggregates, suggesting that it can either be drawn into the aggregates in a nonprion conformation or acquire the prion conformation upon interaction with polyQ. Another possibility is that rare cells with polyQ aggregates observed in the initially [rnq⁻] culture originate from spontaneous generation of the [Rnq⁺], which in turn facilitates aggregation of polyQ.

It is noteworthy that overproduction followed by aggregation of the QN-rich protein Sup35 or its prion-forming domain is toxic to yeast cells containing either [PSI⁺] or [Rnq⁺] prions (8). Remarkably, Sup35 interacts with Sla1 (3), and the toxicity of overproduced Sup35, similar to the toxicity of polyQ, is greatly increased in the *sla1* deletion mutants (Newnam and Chernoff, unpublished data). This suggests that the endocytic pathway may represent a universal target of various protein aggregates in the yeast cell.

Here we also demonstrated that aggregation of polyQ is associated with defects in endocytosis in HEK293 mammalian cells. Indeed, the majority of cells with 103Q aggregates, but not cells without aggregates, showed very poor internalization of transferrin (Fig. 7) (Of note is that we did not observe the endocytosis defects in stably transfected PC-12 cells expressing 103Q, suggesting that the defect may depend on the cell type, levels of 103Q expression, and other factors.) The connection between huntingtin and the endocytic machinery has previously been demonstrated in mammalian cells. In fact, huntingtin was shown to colocalize with endocytic vesicles (51). Furthermore, huntingtin interacts with multiple components of the endocytic machinery and vesicular transport in general (15, 26, 37, 42, 43). Therefore, our results showing that polyQ-induced toxicity is associated with endocytic defects may very well be relevant to neurons. It was previously shown that expression of mutant huntingtin in striatal neurons causes the appearance of multiple vacuoles, which led to the suggestion that endocytosis remains functional and may even be enhanced by huntingtin (22). However, direct measurements of endocytosis

tosis were not done, and accumulation of vacuoles could result from autophagy or other events. Consistent with this, we also found that autophagy proceeded normally in polyQ-expressing cells (see above).

Interestingly, one of the mutations that strongly enhanced polyQ toxicity was deletion of *VPS13* (*SOI1*), which is involved in various steps of vesicular transport (7). Mutation in a human homolog of yeast *VPS13* causes the genetic disease chorea acanthocytosis (36, 49). Besides defects in red blood cells, this disease causes severe brain pathology and behavioral abnormalities similar to those in Huntington's disease (44). These similarities suggest that a common pathway, i.e., vesicular transport, is affected in brains of chorea acanthocytosis and Huntington's disease patients.

Our finding that endocytosis is inhibited by expanded polyQ does not exclude the possibility that there are other, perhaps multiple, effects of polyQ on cell death. A distinct effect of expanded polyQ, described here, is delocalization of actin patches, which results in a disorganization of the actin cytoskeleton. Since many elements of the endocytosis machinery are also involved in organization of cortical actin (for reviews, see references 30 and 40), the described polyQ-related defects of endocytosis may be linked to other actin-dependent functions. However, expression of 103Q did not enhance the cell's sensitivity to Calcofluor white, a compound that inhibits cell wall biosynthesis, and stabilization of the cell wall with sorbitol had no effect on the polyQ toxicity (not shown). These data suggest that cell wall maintenance, another process associated with the actin cytoskeleton, was not as sensitive to 103Q aggregation as was endocytosis. Analogously, budding of yeast cells, which also relies on the actin cytoskeleton, appeared to be unaffected by 103Q expression (25).

Some mutations in endocytosis-related genes are lethal (e.g., *pan1* or *rsp5*). Many others do not cause a loss of viability under normal conditions; however, elevation of temperature or combination of several of such mutations often causes lethality. Therefore, it is conceivable that multiple defects in endocytosis may become a primary source for cell toxicity. In addition to inhibition of endocytosis and effects on the actin cytoskeleton, polyQ aggregation can also cause inhibition of protein degradation (5) and suppression of certain transcription programs (32, 46). Therefore, the actual polyQ toxicity may derive from cumulative defects in all of these systems.

ACKNOWLEDGMENTS

This work was supported by a Hereditary Disease Foundation grant to M.Y.S., by a Burroughs Wellcome Fund New Investigator Award in the Pharmacological Sciences and NIH R01 award GM60979 to B.W., by NSF DBI grant 0099705 to J.M.M. and B.W., and by a grant from the Huntington's Disease Society of America to Y.O.C.

We thank Gary Newnan for help with some experiments. We thank D. Drubin for the gift of the *sla2* strain and J. Huibregtse for the gift of the *Rsp5-HA* strain.

Anatoli B. Meriin and Xiaoqian Zhang contributed equally to this work.

REFERENCES

- Anton, L. C., U. Schubert, I. Bacik, M. F. Princiotto, P. A. Wearsch, J. Gibbs, P. M. Day, C. Realini, M. C. Rechsteiner, J. R. Bennink, and J. W. Yewdell. 1999. Intracellular localization of proteasomal degradation of a viral antigen. *J. Cell Biol.* **146**:113–124.
- Baba, M., M. Osumi, S. V. Scott, D. J. Klionsky, and Y. Ohsumi. 1997. Two distinct pathways for targeting proteins from the cytoplasm to the vacuole/lysosome. *J. Cell Biol.* **139**:1687–1695.
- Bailleul, P. A., G. P. Newnam, J. N. Steenbergen, and Y. O. Chernoff. 1999. Genetic study of interactions between the cytoskeletal assembly protein sla1 and prion-forming domain of the release factor Sup35 (eRF3) in *Saccharomyces cerevisiae*. *Genetics* **153**:81–94.
- Bates, G. P., L. Mangiarini, and S. W. Davies. 1998. Transgenic mice in the study of polyglutamine repeat expansion diseases. *Brain Pathol.* **8**:699–714.
- Bence, N. F., R. M. Sampat, and R. R. Kopito. 2001. Impairment of the ubiquitin-proteasome system by protein aggregation. *Science* **292**:1552–1555.
- Berkower, C., D. Loayza, and S. Michaelis. 1994. Metabolic instability and constitutive endocytosis of STE6, the a-factor transporter of *Saccharomyces cerevisiae*. *Mol. Biol. Cell* **5**:1185–1198.
- Brickner, J. H., and R. S. Fuller. 1997. SOI1 encodes a novel, conserved protein that promotes TGN-endosomal cycling of Kex2p and other membrane proteins by modulating the function of two TGN localization signals. *J. Cell Biol.* **139**:23–36.
- Chernoff, Y. O., S. M. Uptain, and S. L. Lindquist. 2002. Analysis of prion yeast. *Methods Enzymol.* **351**:499–538.
- Davis, N., J. Horecka, and G. J. Sprague. 1993. Cis- and trans-acting functions required for endocytosis of the yeast pheromone receptors. *J. Cell Biol.* **122**:53–65.
- Derkatch, I. L., M. E. Bradley, J. Y. Hong, and S. W. Liebman. 2001. Prions affect the appearance of other prions: the story of [PIN⁺]. *Cell* **106**:171–182.
- Diamond, M. I., M. R. Robinson, and K. R. Yamamoto. 2000. Regulation of expanded polyglutamine protein aggregation and nuclear localization by the glucocorticoid receptor. *Proc. Natl. Acad. Sci. USA* **97**:657–661.
- DiFiglia, M., E. Sapp, K. O. Chase, S. W. Davies, G. P. Bates, J. P. Vonsattel, and N. Aronin. 1997. Aggregation of huntingtin in neuronal intranuclear inclusions and dystrophic neurites in brain. *Science* **277**:1990–1993.
- Fabunmi, R. P., W. C. Wigley, P. J. Thomas, and G. N. DeMartino. 2000. Activity and regulation of the centrosome-associated proteasome. *J. Biol. Chem.* **275**:409–413.
- Garcia-Mata, R., Z. Bebek, E. J. Sorscher, and E. S. Sztul. 1999. Characterization and dynamics of aggresome formation by a cytosolic GFP-chimera. *J. Cell Biol.* **146**:1239–1254.
- Hattula, K., and J. Peranen. 2000. FIP-2, a coiled-coil protein, links Huntingtin to Rab8 and modulates cellular morphogenesis. *Curr. Biol.* **10**:1603–1606.
- Helmuth, L. 2001. Cell biology. Protein clumps hijack cell's clearance system. *Science* **292**:1467–1468.
- Huibregtse, J. M., M. Scheffner, S. Beaudenon, and P. M. Howley. 1995. A family of proteins structurally and functionally related to the E6-AP ubiquitin-protein ligase. *Proc. Natl. Acad. Sci. USA* **92**:5249.
- Humbert, S., E. A. Bryson, F. P. Cordelieres, N. C. Connors, S. R. Datta, S. Finkbeiner, M. E. Greenberg, and F. Saudou. 2002. The IGF-1/Akt pathway is neuroprotective in Huntington's disease and involves Huntingtin phosphorylation by Akt. *Dev. Cell* **2**:831–837.
- Johnston, J. A., C. L. Ward, and R. R. Kopito. 1998. Aggresomes: a cellular response to misfolded proteins. *J. Cell Biol.* **143**:1883–1898.
- Kalchman, M. A., H. B. Koide, K. McCutcheon, R. K. Graham, K. Nichol, K. Nishiyama, P. Kazemi-Esfarjani, F. C. Lynn, C. Wellington, M. Metzler, Y. P. Goldberg, I. Kanazawa, R. D. Gietz, and M. R. Hayden. 1997. HIP1, a human homologue of *S. cerevisiae* Sla2p, interacts with membrane-associated huntingtin in the brain. *Nat. Genet.* **16**:44–53.
- Kaminska, J., B. Gajewska, A. K. Hopper, and T. Zoladek. 2002. Rsp5p, a new link between the actin cytoskeleton and endocytosis in the yeast *Saccharomyces cerevisiae*. *Mol. Cell. Biol.* **22**:6946–6948.
- Kegel, K. B., M. Kim, E. Sapp, C. McIntyre, J. G. Castano, N. Aronin, and M. DiFiglia. 2000. Huntingtin expression stimulates endosomal-lysosomal activity, endosome tubulation, and autophagy. *J. Neurosci.* **20**:7268–7278.
- Kim, S., E. A. Nollen, K. Kitagawa, V. P. Bindokas, and R. I. Morimoto. 2002. Polyglutamine protein aggregates are dynamic. *Nat. Cell Biol.* **4**:826–831.
- Meriin, A. B., K. Mabuchi, V. L. Gabai, J. A. Yaglom, A. Kazantsev, and M. Y. Sherman. 2001. Intracellular aggregation of polypeptides with expanded polyglutamine domain is stimulated by stress-activated kinase mek1. *J. Cell Biol.* **153**:851–864.
- Meriin, A. B., X. Zhang, X. He, G. P. Newnam, Y. O. Chernoff, and M. Y. Sherman. 2002. Huntington toxicity in yeast model depends on polyglutamine aggregation mediated by a prion-like protein Rnq1. *J. Cell Biol.* **157**:997–1004.
- Metzler, M., V. Legendre-Guillemain, L. Gan, V. Chopra, A. Kwok, P. S. McPherson, and M. R. Hayden. 2001. HIP1 functions in clathrin-mediated endocytosis through binding to clathrin and adaptor protein 2. *J. Biol. Chem.* **276**:39271–39276.
- Michelitsch, M. D., and J. S. Weissman. 2000. A census of glutamine/asparagine-rich regions: implications for their conserved function and the prediction of novel prions. *Proc. Natl. Acad. Sci. USA* **97**:11910–11915.
- Mitchell, D. A., T. K. Marshall, and R. J. Deschenes. 1993. Vectors for the inducible overexpression of glutathione S-transferase fusion proteins in yeast. *Yeast* **9**:715–722.
- Morley, J. F., H. R. Brignull, J. J. Weyers, and R. I. Morimoto. 2002. The threshold for polyglutamine-expansion protein aggregation and cellular tox-

- icity is dynamic and influenced by aging in *Caenorhabditis elegans*. *Proc. Natl. Acad. Sci. USA* **99**:10417–10422.
30. Munn, A. L. 2001. Molecular requirements for the internalisation step of endocytosis: insights from yeast. *Biochim. Biophys. Acta* **1535**:236–257.
 31. Noda, T., K. Suzuki, and Y. Ohsumi. 2002. Yeast autophagosomes: de novo formation of a membrane structure. *Trends Cell Biol.* **12**:231–235.
 32. Nucifora, F. C., Jr., M. Sasaki, M. F. Peters, H. Huang, J. K. Cooper, M. Yamada, H. Takahashi, S. Tsuji, J. Troncoso, V. L. Dawson, T. M. Dawson, and C. A. Ross. 2001. Interference by huntingtin and atrophin-1 with cbp-mediated transcription leading to cellular toxicity. *Science* **291**:2423–2428.
 33. Osherovich, L. Z., and J. S. Weissman. 2001. Multiple Gln/Asn-rich prion domains confer susceptibility to induction of the yeast [PSI(+)] prion. *Cell* **106**:183–194.
 34. Peters, P. J., K. Ning, F. Palacios, R. L. Boshans, A. Kazantsev, L. M. Thompson, B. Woodman, G. P. Bates, and C. D'Souza-Schorey. 2002. Arfap12 regulates the aggregation of mutant huntingtin protein. *Nat. Cell Biol.* **4**:240–245.
 35. Pruyn, D., and A. Bretscher. 2000. Polarization of cell growth in yeast. *J. Cell Sci.* **113**:571–585.
 36. Rampoldi, L., C. Dobson-Stone, J. P. Rubio, A. Danek, R. M. Chalmers, N. W. Wood, C. Verellen, X. Ferrer, A. Malandrini, G. M. Fabrizi, R. Brown, J. Vance, M. Pericak-Vance, G. Rudolf, S. Carre, E. Alonso, M. Manfredi, A. H. Nemeth, and A. P. Monaco. 2001. A conserved sorting-associated protein is mutant in chorea-acanthocytosis. *Nat. Genet.* **28**:119–120.
 37. Rao, D. S., J. C. Chang, P. D. Kumar, I. Mizukami, G. M. Smithson, S. V. Bradley, A. F. Parlow, and T. S. Ross. 2001. Huntingtin interacting protein 1 is a clathrin coat binding protein required for differentiation of late spermatogenic progenitors. *Mol. Cell Biol.* **21**:7796–7806.
 38. Rieder, S. E., L. M. Banta, K. Kohrer, J. M. McCaffery, and S. D. Emr. 1996. Multilamellar endosome-like compartment accumulates in the yeast vps28 vacuolar protein sorting mutant. *Mol. Biol. Cell* **7**:985–999.
 39. Scherzinger, E., R. Lurz, M. Turmaine, L. Mangiarini, B. Hollenbach, R. Hasenbank, G. P. Bates, S. W. Davies, H. Lehrach, and E. E. Wanker. 1997. Huntingtin-encoded polyglutamine expansions form amyloid-like protein aggregates in vitro and in vivo. *Cell* **90**:549–558.
 40. Schott, D., T. Huffaker, and A. Bretscher. 2002. Microfilaments and microtubules: the news from yeast. *Curr. Opin. Microbiol.* **5**:564–574.
 41. Sherman, M. Y., and A. L. Goldberg. 2001. Cellular defenses against unfolded proteins: a cell biologist thinks about neurodegenerative diseases. *Neuron* **29**:15–32.
 42. Singaraja, R. R., S. Hadano, M. Metzler, S. Givan, C. L. Wellington, S. Warby, A. Yanai, C. A. Gutekunst, B. R. Leavitt, H. Yi, K. Fichter, L. Gan, K. McCutcheon, V. Chopra, J. Michel, S. M. Hersch, J. E. Ikeda, and M. R. Hayden. 2002. HIP14, a novel ankyrin domain-containing protein, links huntingtin to intracellular trafficking and endocytosis. *Hum. Mol. Genet.* **11**:2815–2828.
 43. Sittler, A., S. Walter, N. Wedemeyer, R. Hasenbank, E. Scherzinger, H. Eickhoff, G. P. Bates, H. Lehrach, and E. E. Wanker. 1998. SH3GL3 associates with the Huntingtin exon 1 protein and promotes the formation of polyglu-containing protein aggregates. *Mol. Cell* **2**:427–436.
 44. Sotaniemi, K. A. 1983. Choreia-acanthocytosis. Neurological disease with acanthocytosis. *Acta Neurol. Scand.* **68**:53–56.
 45. Steffan, J. S., L. Bodai, J. Pallos, M. Poelman, A. McCampbell, B. L. Apostol, A. Kazantsev, E. Schmidt, Y. Z. Zhu, M. Greenwald, R. Kurokawa, D. E. Housman, G. R. Jackson, J. L. Marsh, and L. M. Thompson. 2001. Histone deacetylase inhibitors arrest polyglutamine-dependent neurodegeneration in *Drosophila*. *Nature* **413**:739–743.
 46. Steffan, J. S., A. Kazantsev, O. Spasic-Boskovic, M. Greenwald, Y. Z. Zhu, H. Gohler, E. E. Wanker, G. P. Bates, D. E. Housman, and L. M. Thompson. 2000. The Huntington's disease protein interacts with p53 and CREB-binding protein and represses transcription. *Proc. Natl. Acad. Sci. USA* **97**:6763–6768.
 47. Tang, H., A. Munn, and M. Cai. 1997. EH domain proteins Pan1p and End3p are components of a complex that plays a dual role in organization of the cortical actin cytoskeleton and endocytosis in *Saccharomyces cerevisiae*. *Mol. Cell Biol.* **17**:4294–4304.
 48. Tang, H. Y., J. Xu, and M. Cai. 2000. Pan1p, End3p, and Sla1p, three yeast proteins required for normal cortical actin cytoskeleton organization, associate with each other and play essential roles in cell wall morphogenesis. *Mol. Cell Biol.* **20**:12–25.
 49. Ueno, S., Y. Maruki, M. Nakamura, Y. Tomemori, K. Kamae, H. Tanabe, Y. Yamashita, S. Matsuda, S. Kaneko, and A. Sano. 2001. The gene encoding a newly discovered protein, chorein, is mutated in chorea-acanthocytosis. *Nat. Genet.* **28**:121–122.
 50. van Dam, E. M., T. ten Broeke, K. Jansen, P. Spijkers, and W. Stoorvogel. 2002. Endocytosed transferrin receptors recycle via distinct dynamin and phosphatidylinositol 3-kinase-dependent pathways. *J. Biol. Chem.* **277**:48876–48883.
 51. Velier, J., M. Kim, C. Schwarz, T. W. Kim, E. Sapp, K. Chase, N. Aronin, and M. Difiglia. 1998. Wild-type and mutant huntingtins function in vesicle trafficking in the secretory and endocytic pathways. *Exp. Neurol.* **152**:34–40.
 52. Vida, T. A., and S. D. Emr. 1995. A new vital stain for visualizing vacuolar membrane dynamics and endocytosis in yeast. *J. Cell Biol.* **128**:779–792.
 53. Vidair, C. A., R. N. Huang, and S. J. Doxsey. 1999. Heat shock causes protein aggregation and reduced protein solubility at the centrosome and other cytoplasmic locations. *Int. J. Hyperthermia* **12**:681–695.
 54. Wang, G., J. M. McCaffery, B. Wendland, S. Dupre, R. Haguener-Tsapis, and J. M. Huibregtse. 2001. Localization of the Rsp5p ubiquitin-protein ligase at multiple sites within the endocytic pathway. *Mol. Cell Biol.* **21**:3564–3575.
 55. Warren, D., P. Andrews, C. Gourlay, and K. Ayscough. 2002. Sla1p couples the yeast endocytic machinery to proteins regulating actin dynamics. *J. Cell Sci.* **115**:1703–1715.
 56. Wendland, B., and S. Emr. 1998. Pan1p, yeast eps15, functions as a multivalent adaptor that coordinates protein-protein interactions essential for endocytosis. *J. Cell Biol.* **141**:71–84.
 57. Wendland, B., J. M. McCaffery, Q. Xiao, and S. D. Emr. 1996. A novel fluorescence-activated cell sorter-based screen for endocytosis mutants identifies a yeast homologue of mammalian eps15. *J. Cell Biol.* **135**:1485–1500.
 58. Wigley, W. C., R. P. Fabunmi, M. G. Lee, C. R. Marino, S. Muallem, G. N. DeMartino, and P. J. Thomas. 1999. Dynamic association of proteasomal machinery with the centrosome. *J. Cell Biol.* **145**:481–490.
 59. Winzler, E. A., D. D. Shoemaker, A. Astromoff, H. Liang, K. Anderson, B. Andre, R. Bangham, R. Benito, J. D. Boeke, H. Bussey, A. M. Chu, C. Connelly, K. Davis, F. Dietrich, S. W. Dow, M. El Bakkoury, F. Foury, S. H. Friend, E. Gentalen, G. Giaever, J. H. Hegemann, T. Jones, M. Laub, H. Liao, R. W. Davis, et al. 1999. Functional characterization of the *S. cerevisiae* genome by gene deletion and parallel analysis. *Science* **285**:901–906.
 60. Wojcik, C., D. Schroeter, S. Wilk, J. Lamprecht, and N. Paweletz. 1996. Ubiquitin-mediated proteolysis centers in HeLa cells—indication from studies of an inhibitor of the chymotrypsin-like activity of the proteasome. *Eur. J. Cell Biol.* **71**:311–318.
 61. Yang, S., M. J. Cope, and D. G. Drubin. 1999. Sla2p is associated with the yeast cortical actin cytoskeleton via redundant localization signals. *Mol. Biol. Cell* **10**:2265–2283.
 62. Young, A. 1998. Huntington's disease and other trinucleotide repeat disorders. Scientific American, Inc., New York, N.Y.
 63. Zeng, G., X. Yu, and M. Cai. 2001. Regulation of yeast actin cytoskeleton-regulatory complex Pan1p/Sla1p/End3p by serine/threonine kinase Prk1p. *Mol. Biol. Cell* **12**:3759–3772.